

Ion-Imprinted PHEMA Based Monolith for the Removal of Fe³⁺ Ions from Aqueous Solutions

Serpil Özkara,¹ Müge Andaç,¹ Veyis Karakoç,¹ Rıdvan Say,² Adil Denizli¹

¹Department of Chemistry, Biochemistry Division, Hacettepe University, Ankara, Turkey

²Department of Chemistry, Anadolu University, Eskisehir, Turkey

Received 5 April 2010; accepted 12 September 2010

DOI 10.1002/app.33400

Published online 1 December 2010 in Wiley Online Library (wileyonlinelibrary.com).

ABSTRACT: Molecular recognition based Fe³⁺ imprinted monolith was prepared for selective removal of Fe³⁺ ions from aqueous solutions. The precomplexation was achieved by the coordination of Fe³⁺ ions with *N*-methacryloyl-(L)-cysteine methyl ester (MAC) to form the complex monomer (MAC-Fe³⁺). The polymerization step was then carried out in the presence of MAC-Fe³⁺ complex and hydroxyethyl methacrylate (HEMA) monomer by bulk polymerization to constitute a Fe³⁺-imprinted polymer (PHEMAC-Fe³⁺). The specific surface area of PHEMAC-Fe³⁺ monolith was found to be 35.2 m²/g, with a swelling ratio of 60.2% after the template was removed from the monolith by 0.1M EDTA solution. The maximum adsorption capacity of PHEMAC-

Fe³⁺ monolith for Fe³⁺ ion was 0.76 mg/g. The adsorption behavior of the monolith has been successfully described by the Langmuir isotherm. It was determined that the relative selectivity of PHEMAC-Fe³⁺ monolith was 59.7 and 37.0 times greater than that of the nonimprinted PHEMAC monolith as compared with the Cd²⁺ and Ni²⁺ ions, respectively. The PHEMAC-Fe³⁺ monolith was recovered and reused many times without any significant decrease in its adsorption capacity. © 2010 Wiley Periodicals, Inc. *J Appl Polym Sci* 120: 1829–1836, 2011

Key words: molecular imprinting; monolith; molecular recognition; iron removal

INTRODUCTION

Molecular imprinting has become an attractive technology to create recognition sites in a macromolecular matrix over the past decades.^{1–3} Molecularly imprinted polymers (MIPs) were synthetically prepared by interactive complexation of a functional monomer with a template, followed by polymerization with a crosslinker. The template was removed from the polymer matrix to form cavities sculpted around the template molecules that are complementary in size, shape, and orientation to those of the template.⁴ MIPs are easy to prepare, stable, inexpensive, and capable of molecular recognition. Therefore, MIPs can be considered as artificial affinity media. Separation techniques established based on the principles of molecular recognition has received much attention in various fields because of the high selectivity they exhibit towards target molecules.^{5–7} In an ion-imprinting process, the selectivity of an imprinted polymeric adsorbent relies on the coordination, the charge, and the size of the ion being targeted.^{8–12} The methodology describing in detail metal ion adsorption have been extensively reported in literature.^{13–19}

Conventional packed-bed columns possess some inherent limitations such as a slow diffusional mass transfer and a large void volume that may form among the polymeric beads packed in the column.²⁰ Although some new stationary phases such as non-porous polymeric beads²¹ and perfusion chromatography packings have been designed to circumvent the aforementioned problems, these limitations yet cannot be fully resolved.²² The most recent generation of monolith materials are considered in the separation science as novel types of stationary phases because of the ease of their preparations, their excellent flow properties, and the high performance they exhibit in comparison to the conventional beads used in the separation of biomolecules.²³ Alternatively, porous monoliths are known to have several advantage points in bioseparation, e.g., they have large surface area, short diffusion path, and low pressure drop for adsorption and elution.²⁴

In this article, the Fe³⁺-imprinted PHEMAC monolithic column was prepared by *in situ* polymerization where there is no need to grind and sieve to form particles for column packing. The Fe³⁺-imprinted PHEMAC monolithic column was characterized and used for selective removal of Fe³⁺ ions from aqueous solution. In addition, the adsorption capacity of PHEMAC-Fe³⁺ for Fe³⁺ and its competitive Fe³⁺ binding in the presence of Fe²⁺, Cd²⁺, and Ni²⁺ are reported and discussed here. Finally, the recoverability and reusability of PHEMAC-Fe³⁺ are evaluated in the last section.

Correspondence to: A. Denizli (denizli@hacettepe.edu.tr).

EXPERIMENTAL

Materials

Hydroxyethyl methacrylate (HEMA) and ethylene glycol dimethacrylate (EGDMA) were obtained from Fluka A.G. (Buchs, Switzerland), distilled under reduced pressure in the presence of hydroquinone inhibitor, and stored at 4°C until use. L-Cysteine methylester and methacryloyl chloride were purchased from Sigma (St. Louis, USA). *N,N,N',N'*-tetramethylene diamine (TEMED) was obtained from Fluka A.G. (Buchs, Switzerland). All other chemicals were of reagent grade and purchased from Merck AG (Darmstadt, Germany).

Preparation and characterization of PHEMAC-Fe³⁺ monolith

The preparation and characterization of the *N*-methacryloyl-(L)-cysteinemethylester (MAC) was adapted from the procedure reported elsewhere.²⁵ The complex monomer, MAC-Fe³⁺, was prepared by slow addition of solid *N*-methacryloyl-(L)-cysteinemethylester (MAC) (2.0 mmol) into 15 mL solution of ethanol–water mixture (50/50 *v/v*) in a vessel, followed by dissolution of iron nitrate (Fe(NO₃)₂·9H₂O) (1.0 mmol) at room temperature by constant stirring (250 rpm) for 3 h. The newly generated (fresh) monomer–metal complex (MAC-Fe³⁺) was filtered off, washed with 99% ethanol, and dried in a vacuum oven at 50°C for 24 h.

PHEMAC and PHEMAC-Fe³⁺ monoliths were prepared in a glass tube by an *in situ* polymerization process in the presence of H₂O₂/TEMED (the initiator) and acetonitrile (the porogenic diluent or the pore former).²⁵ The initiator H₂O₂/TEMED was dissolved in a mixture of HEMA (200 μL), EGDMA (400 μL), MAC-Fe³⁺ (40 mg), and acetonitrile (600 μL). The monomer mixture including the initiator and the porogenic diluent was then purged with nitrogen gas for 15 min. The resulting solution was finally transferred into a glass tube (10 cm in length and 10 mm inner diameter) and sealed off with parafilm. The polymerization was allowed to proceed at 60°C in a water bath for 4 h followed by another 2 h of an extended reaction at 75°C. After the polymerization was completed, the unreacted monomers and the porogenic diluent were removed by pumping through the column first by ethyl alcohol (50 mL) and then water (50 mL) at a flow rate of 1.0 mL/min. The template ion Fe³⁺ trapped in the polymer monolith was removed by pumping with 0.1M EDTA solution through the monolithic column. The monolith, free of Fe³⁺, was finally rinsed with 0.1M HNO₃ solution. The refined PHEMAC-Fe³⁺ was stored at 4°C in buffer containing 0.02% sodium azide until use. As a control, a nonimprinted monolith

(PHEMAC) was also prepared in the absence of template ions by the same polymerization procedure used to prepare PHEMAC-Fe³⁺. All physical and chemical properties of MAC monomer, MAC-Fe³⁺ complex monomer, PHEMAC-Fe³⁺, and PHEMAC monolith were characterized and profoundly discussed in our previous study.²⁵ The surface structures of the monoliths (PHEMAC and PHEMAC-Fe³⁺) were visualized and examined by scanning electron microscopy (SEM). After the monolith samples were dried in a vacuum oven at 50°C for 24 h, tiny fragments of the monoliths were mounted on SEM sample holders on which they were sputter-coated for 2 min. The samples were then consecutively mounted in a scanning electron microscope (Model: JSM 5600, Jeol, Japan) to visualize the surface structures of each monolith at desired magnification levels.

The elemental analysis of monolith was implemented on a Leco Elemental Analyzer (Model CHNS-932, USA) to evaluate the MAC incorporation amount from the sulfur stoichiometry in the monolith. Porosity of the PHEMAC-Fe³⁺ monolith was measured by a N₂ gas sorption technique, performed on Flowsorb II, (Micromeritics Instrument Corp., Norcross, USA). The specific surface area of PHEMAC-Fe³⁺ in dry state was determined by multipoint Brunauer-Emmett-Teller (BET) apparatus (Quantachrome, Nova 2200E). PHEMAC-Fe³⁺ (0.5 g) was placed in the sample holder of BET and degassed by passing through N₂-gas at 150°C for 1 h. The adsorption of the N₂ gas was performed at –210°C, whereas desorption was performed at room temperature. Experimental values obtained from desorption step was used to calculate the specific surface area of the monolith. Pore volumes and an average pore diameter for PHEMAC-Fe³⁺ were determined by the method on a BJH (Barrett, Joyner, Halenda) model.

Fe³⁺ adsorption in aqueous solutions

Fe³⁺ adsorption onto the PHEMAC-Fe³⁺ monolith in aqueous solutions was studied in a continuous system. The effect of flow rate on Fe³⁺ adsorption was implemented in the range of 0.5–3.5 mL/min. The pH of the solution was changed between pH 3.0 and pH 5.0 to determine the effect of pH. The effect of the equilibrium concentration on Ni²⁺ ion adsorption was studied in the range of 5–100 mg/L.

The Fe³⁺ removal tests were conducted on aqueous solutions via PHEMAC and the PHEMAC-Fe³⁺ monolithic columns. The monolithic column, both equipped with a water jacket for temperature control, were degassed under reduced pressure by a water suction pump. The monolithic column was then equilibrated by passing through four column volumes of phosphate buffer adjusted at pH 7.4. Then, 50 mL of the aqueous solution was passed

through the monolithic column at moderate pressure by a peristaltic pump over 2 h. The Fe³⁺ ion captured by the monolithic column was eluted by a solution of 0.1M EDTA. The concentration of Fe³⁺ in the eluted phase was determined by a graphite furnace atomic absorption (GFAA) spectrophotometer (Analyst 800/Perkin–Elmer, USA) using a deuterium background correction and a spectral bandwidth of 0.5 nm. A hollow cathode iron lamp was used in the spectrophotometer to detect Fe³⁺ at a current/wavelength of 8.0 mA/248.3 nm. The instrument response was periodically checked with known Fe³⁺ solution standards. Each set of the iron removal experiments was repeated three times to determine mean values and their standard deviations by the standard statistical method. A confidence interval of 95% was taken into account to determine the error limit of each data set. The amount of Fe³⁺ adsorbed on a unit mass of each monolith was evaluated by using a mass balance approach. The amount of Fe³⁺ adsorption per unit mass of the monolith was evaluated by eq. (1).

$$Q = [(C_o - C)V]/m \quad (1)$$

Here, Q is the amount of Fe³⁺ ions adsorbed onto unit mass of the monolith (mg/g); C_o and C are the concentrations of the Fe³⁺ ions in the initial solution and in the aqueous phase after treatment for certain period of time, respectively, (mg/L); V is the volume of the solution (L); and m is the mass of the monolith used (g).

Selectivity experiments

The specificity of PHEMAC-Fe³⁺ monolith towards Fe³⁺ was assessed by competitive adsorption studies in the presence of Fe³⁺/Fe²⁺, Fe³⁺/Cd²⁺, and Fe³⁺/Ni²⁺ ion pairs. The binary mixtures including Fe²⁺, Cd²⁺, or Ni²⁺ were then separately treated with PHEMAC-Fe³⁺ and PHEMAC monolith. After a competitive adsorption equilibrium was reached, the concentration of Fe³⁺, Cd²⁺, and Ni²⁺ in the binary mixtures were detected by GFAA spectroscopy using the same equipment and instrument parameters described in previous section.

Distribution coefficients of (K_d) for Fe²⁺, Cd²⁺, and Ni²⁺ with respect to Fe³⁺ were calculated by eq. (2).²⁶

$$K_d = [(C_i - C_f)C_f] \times V/m \quad (2)$$

where K_d (mL/g) is a distribution coefficient for the competing metal ion. C_i and C_f are the initial and the final concentrations of metal ions (mg/L), respectively. V is the volume of the solution mixture (mL) and m is the mass of monolith (g).

The generic term in eq. (3) was adopted to determine a selectivity coefficient (k) for the binding of

Fe³⁺ onto the PHEMAC-Fe³⁺ monolith in the presence of a competing species such as Fe²⁺, Cd²⁺, and Ni²⁺, in which $K_{d(\text{competing metal ion})}$ is the distribution coefficient of the competing metal ion.

$$k = K_{d(\text{template metal ion})}/K_{d(\text{competing metal ion})} \quad (3)$$

A ratio of the selectivity coefficients (k') in eq. (4), in which $k_{\text{imprinted}}$ is for the imprinted monolith (PHEMAC-Fe³⁺) in the presence of the Fe³⁺/Fe²⁺, Fe³⁺/Cd²⁺, or the Fe³⁺/Ni²⁺ ion pairs and k_{control} is for the nonimprinted monolith (PHEMAC) in the presence of the Fe³⁺/Fe²⁺, Fe³⁺/Cd²⁺, or the Fe³⁺/Ni²⁺ ion pairs was used as an approximation to assess the effect of imprinting on ion selectivity.

$$k' = k_{\text{imprinted}}/k_{\text{control}} \quad (4)$$

Desorption and reusability

Fe³⁺ bound to PHEMAC-Fe³⁺ monolithic column was desorbed by recirculating a desorbing agent, a solution of 0.1M EDTA through the monolithic column. In a typical desorption procedure, 50 mL of desorption agent was recirculated through the PHEMAC-Fe³⁺ monolith at room temperature for 1 h. The final Fe³⁺ concentration in desorption medium was determined by GFAA spectroscopy. Desorption ratio for Fe³⁺ was calculated based on the ratio of Fe³⁺ released and Fe³⁺ adsorbed. To evaluate the reusability of the PHEMAC-Fe³⁺ column, the Fe³⁺ adsorption–desorption cycle was repeated ten times for the same PHEMAC-Fe³⁺ column, provided that the column was rinsed with a solution of 50 mM NaOH after each desorption procedure to ensure a sterile reusability.

RESULTS AND DISCUSSION

Characterization studies

Specific surface area, total pore volume, and average pore diameter of PHEMAC and PHEMAC-Fe³⁺ monolith are presented in Table I. The specific surface area of PHEMAC-Fe³⁺ was determined by a multipoint BET apparatus to be 35.2 m²/g polymer. The sizes of the pores on PHEMAC-Fe³⁺ were determined via a BJH instrument to average out to 37.4 Å in diameter, in which the pore diameters range from 20 to 245 Å, suggesting the presence of mesopores on the surface of PHEMAC-Fe³⁺. This pore diameter is possibly in the range of diffusion of Fe³⁺ ions. Considering the ionic radius of Fe³⁺ (64 pm), then the mesopores on PHEMAC-Fe³⁺ are said to be sufficiently large to accommodate Fe³⁺ ions. The equilibrium

TABLE I
Physical Properties of PHEMAC and PHEMAC-Fe³⁺ Monolith

Polymer	Surface area ^a (m ² /g)	Total pore volume ^b (mL/g)	Average pore diameter ^c (Å)
PHEMAC	12.2	0.038	22.0
PHEMAC-Fe ³⁺	35.2	0.078	37.4

^a Determined using multipoint BET method.

^b BJH cumulative desorption pore volume of pores between 20 and 245 Å.

^c BJH desorption average pore diameter of pores between 20 and 245 Å.

swelling ratios for PHEMAC and PHEMAC-Fe³⁺ were found to be 60.4% and 60.2%, respectively.

The surface structure of the PHEMAC-Fe³⁺ monolith was visualized by SEM, which is presented at different magnification scales in Figure 1. It is clearly seen in Figure 1 that PHEMAC-Fe³⁺ is composed of much smaller particles, which was polymerized at irregular sizes with many mesopores visible on the surface structure. The PHEMAC-Fe³⁺ monolith was also determined to have better flow properties with a back pressure drop at 4.7 mPa at a flow rate of 1.0 mL/min.

The incorporation of the MAC using sulfur stoichiometry was determined to be 69.4 and 59.2 μmol/g polymer for PHEMAC-Fe³⁺ and PHEMAC

monoliths, respectively. Note that HEMA and other chemicals used in the polymerization process do not contain sulfur. The amount of sulfur determined by elemental analysis originated from only incorporated MAC groups into the polymeric structure.

Fe³⁺ adsorption in aqueous solutions

Effect of flow rate

The adsorption capacity at different flow rates is given in Figure 2. Results show that the adsorption capacity decreased significantly with the increase of the flow rate. This is due to the decrease in contact time between the metal ions and the PHEMAC monolith at higher flow rates. When the flow rate decreases the contact time in the monolithic column is longer, and pore diffusion then becomes effective. Thus, metal ions have more time to diffuse the porous monolithic column and a better adsorption capacity is obtained.

Effect of Fe³⁺ concentration

The adsorption results obtained from via the adsorption experiments based on the binding of Fe³⁺ onto the PHEMAC and PHEMAC-Fe³⁺ monoliths in a series of media containing different equilibrium concentrations

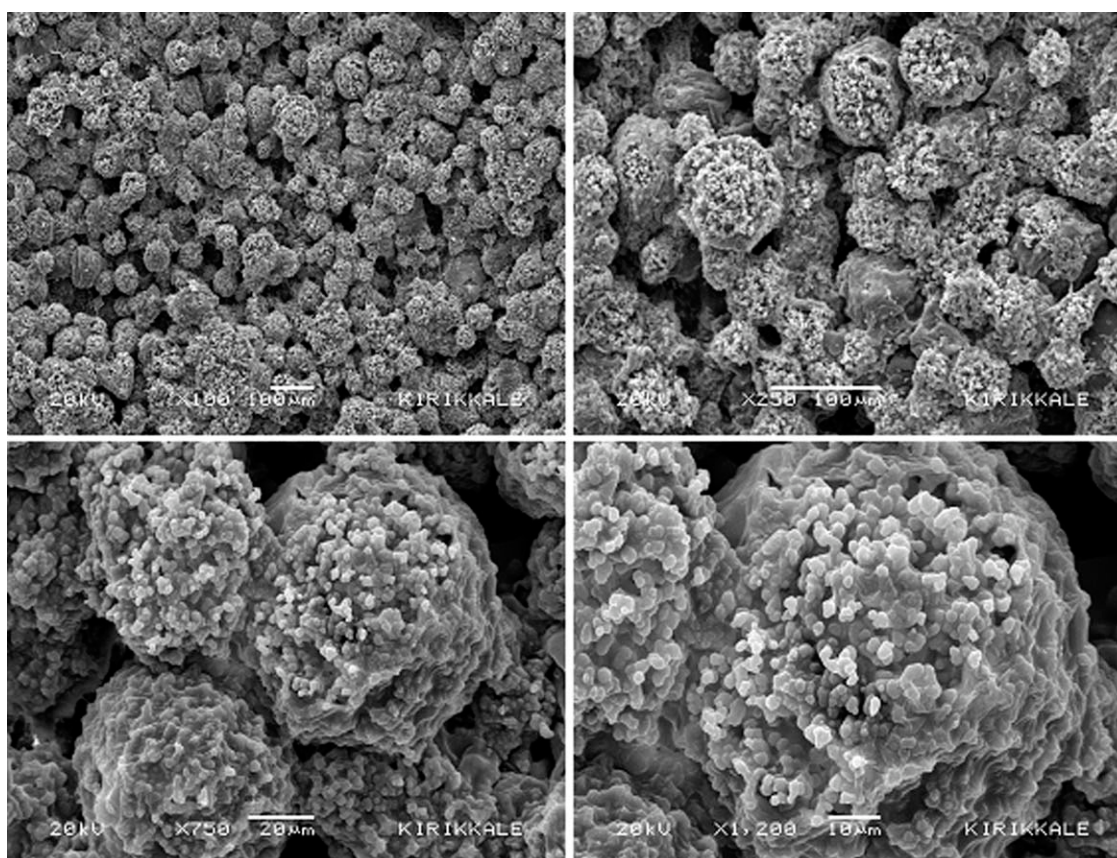


Figure 1 SEM photographs of PHEMAC-Fe³⁺ monolith with different magnifications.

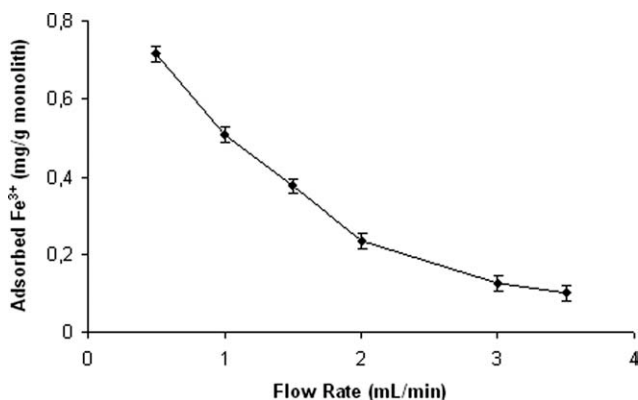


Figure 2 Effect of flow rate on Fe³⁺ adsorption. Experimental conditions are running buffer, 0.1M acetate buffer; pH 5.0; Fe³⁺ concentration, 30 mg/L; V_{total}, 50 mL; m_{monolith}, 0.35 g; T, 20°C.

of Fe³⁺ were plotted in an isotherm in Figure 3. As seen in Figure 3, the Fe³⁺ adsorption linearly increases as the Fe³⁺ concentration in media is increased upto 40 mg/L, after which any further increment in the Fe³⁺ concentration saturates the active binding cavities on PHEMAC-Fe³⁺. The maximum amount of Fe³⁺ adsorbed by PHEMAC-Fe³⁺ was found to be 0.76 mg/g. It should be noted that the nonspecific binding of Fe³⁺ to PHEMAC monolith was very low (5.8 µg/g).

Two important physicochemical aspects for evaluation of the adsorption process as a unit operation are the kinetics and the equilibria of adsorption. Modeling of the equilibrium data has been done using the Langmuir and Freundlich isotherms.²⁷ The Langmuir and Freundlich isotherms are represented as follows, in eqs. (5) and (6), respectively.

$$q = q_{max} \cdot b \cdot \frac{C_e}{(1 + b \cdot C_e)} \quad (5)$$

$$q = K_F \cdot C_e^{1/n} \quad (6)$$

where, *q* is the adsorption capacity (mg/g), *C_e* is the equilibrium Ni²⁺ concentration (mg/mL), *b* is the Langmuir adsorption equilibrium constant (mL/mg) that indicates the monolayer adsorption, *K_F* is the Freundlich constant, and 1/*n* is the Freundlich exponent which represents the heterogeneity of the system. The Freundlich isotherm describes reversible adsorption and is not restricted to the formation of the monolayer.

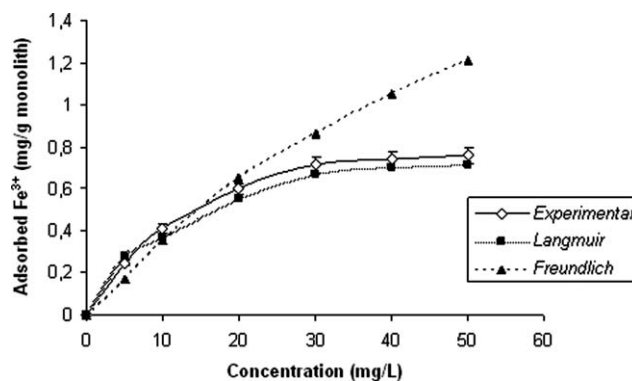


Figure 3 Experimental data for Fe³⁺ absorption fitted to Langmuir and Freundlich isotherms, respectively. Experimental conditions are running buffer: 0.1M acetate buffer; pH 5.0; flow rate, 0.5 mL/min; V_{total}, 50 mL; m_{monolith}, 0.35 g; T, 20°C.

The experimental and calculated results were shown in Table II. The experimental data tend to agree more with a Langmuir adsorption fit rather than Freundlich isotherm, since the correlation coefficient (*R*²) was high (0.99). The maximum amount of adsorption (0.76 mg/g) obtained from experimental results is also very close to the calculated Langmuir adsorption capacity (0.92 mg/g). The Langmuir and Freundlich constants with the correlation coefficients are given in Table II.

In Figure 3, the experimental adsorption behavior was compared with Langmuir and Freundlich adsorption isotherms. The increasing trend in the binding isotherm in Figure 3 confirms the binding cavities formed by the ion-imprinting technique applied in our work. It can be concluded that the adsorbed Fe³⁺ ions onto the PHEMAC-Fe³⁺ monolith shows a monolayer adsorption behavior.

Effect of pH

The metal ion complexation of polymeric ligands and speciation are highly dependent on the equilibrium pH of the medium. In the present study, we changed the pH range between 2.0 and 5.0. The effect of pH on the Fe³⁺ binding of the PHEMAC-Fe³⁺ monolith was shown in Figure 4. As seen here, binding of Fe³⁺ ions increased with increasing pH and then reached almost a plateau value around pH 4.0. The increasing pH of the solution favors complex formation between the sulfydryl groups of

TABLE II
Langmuir and Freundlich Isotherm Constants for PHEMAC-Fe³⁺ Monolith

Notation for monolith	Experimental	Langmuir constants			Freundlich constants		
	<i>q_{ex}</i> (mg/g)	<i>q_{max}</i> (mg/g)	<i>b</i> (mL/mg)	<i>R</i> ²	<i>K_F</i> (mg/g)	<i>n</i>	<i>R</i> ²
PHEMAC-Fe ³⁺	0.76	0.92	118.57	0.99	3.27	2.31	0.95

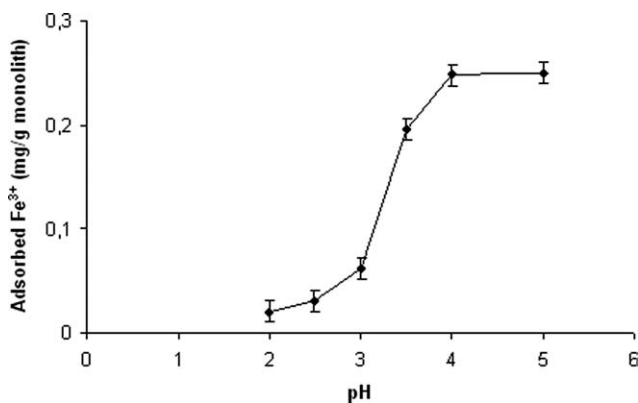


Figure 4 Effect of pH on Fe^{3+} adsorption. Experimental conditions are running buffer, 0.1M acetate buffer; T , 20°C; flow rate, 0.5 mL/min; Fe^{3+} concentration, 5.0 mg/L; V_{total} , 50 mL; $m_{\text{dry monolith}}$, 0.35 g.

MAC in the ion cavities and Fe^{3+} ions. The specific adsorption of Fe^{3+} ions via the MAC groups was pH dependent. Fe^{3+} binding around pH 2.0–2.5 was low, maybe because of protonation of the functional groups on the MAC structure. High binding at increasing pH values shows that Fe^{3+} ions interact with MAC groups by chelating and ion-exchange.

Selectivity experiments

The specificity of PHEMAC- Fe^{3+} for Fe^{3+} in the presence of Fe^{2+} , Cd^{2+} , or Ni^{2+} was determined by a competitive adsorption experiment that was carried out in aqueous solutions under equilibrium conditions. Table III outlines K_d , k , and k' values for Fe^{2+} , Cd^{2+} , and Ni^{2+} with respect to Fe^{3+} , in which case a control monolith PHEMAC was used in parallel to the active monolith (PHEMAC- Fe^{3+}). As seen in Table III, the K_d values determined for Fe^{3+} are significantly higher than those obtained for Fe^{2+} , Cd^{2+} , and Ni^{2+} in both PHEMAC and PHEMAC- Fe^{3+} cases. The selectivity coefficient (k) is inversely related to a competitive affinity binding of an ion (molecule) competing with the template ion (molecule) for the same binding site on the monolith. In regards to the highest binding affinities of Fe^{2+} , Cd^{2+} , and Ni^{2+} to PHEMAC, because of their higher

TABLE III
 K_d , k , and k' Values of Fe^{2+} , Cd^{2+} , and Ni^{2+} With Respect to Fe^{3+}

Metal ion	PHEMAC		PHEMAC- Fe^{3+}		k'
	K_d (mL/g)	k	K_d (mL/g)	k	
Fe^{3+}	0.58	–	2.86	–	–
Fe^{2+}	0.22	2.65	0.04	65.6	24.8
Cd^{2+}	0.54	1.24	0.05	45.9	37.0
Ni^{2+}	0.45	1.07	0.05	63.6	59.7

Metal ion concentration is 30 mg/L, for all metal ions.

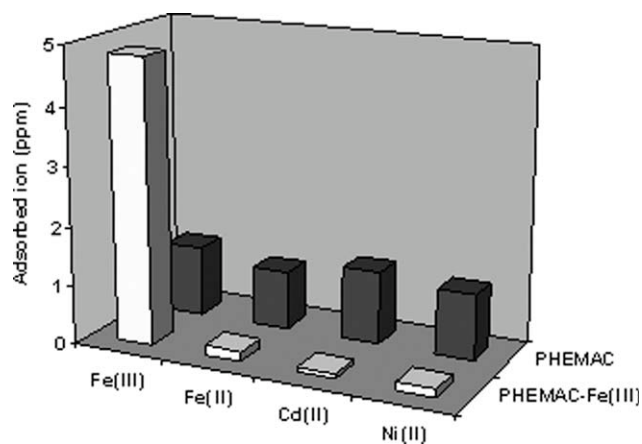


Figure 5 Adsorbed template and competitive ions both in PHEMAC and PHEMAC- Fe^{3+} monoliths for the template/competitive ion pairs (i.e., $\text{Fe}^{3+}/\text{Fe}^{2+}$). Experimental conditions are flow rate, 0.5 mL/min; ion concentration, 30 mg/L; pH, 5.0; V_{total} , 50 mL; $m_{\text{dry monolith}}$, 0.35 g; T , 20°C.

k values compared to those obtained with the control, it is concluded that Fe^{2+} , Cd^{2+} , and Ni^{2+} show relatively high binding affinity to the mesopores on PHEMAC- Fe^{3+} . Results showed that the ion cavities formed in the PHEMAC- Fe^{3+} recognized preferentially Fe^{3+} , indicating that ion cavities matched the size of Fe^{3+} better than Fe^{2+} , Cd^{2+} , and Ni^{2+} . The formation of a coordination complex between the thiol group in the MAC structure and Fe^{3+} is also considered to be another binding mode. The ratio of the k values, the relative selectivity coefficients obtained with PHEMAC- Fe^{3+} and PHEMAC were found to be 24.8, 37.0, and 59.7 (Table III) in the presence of the $\text{Fe}^{3+}/\text{Fe}^{2+}$, $\text{Fe}^{3+}/\text{Cd}^{2+}$, and the $\text{Fe}^{3+}/\text{Ni}^{2+}$ ion couples, respectively.

Figure 5 is a chart showing the amount of the adsorbed ion on PHEMAC and PHEMAC- Fe^{3+} in the presence of competing ions. As seen in Figure 5, Fe^{3+} adsorption is the greatest on PHEMAC- Fe^{3+} . In general, a significant increase is observed in the selectivity of ion-imprinted monoliths when the adsorbent is prepared in the presence of the target ion, a chemical process that is known to be associated with the formation of suitable recognition sites on the monolith.

Desorption and reusability

The regeneration of an ion-imprinted adsorbent is crucial in terms of increasing its industrial efficiency at low costs.^{28,29} Thus, bound Fe^{3+} was desorbed out of the mesopores of PHEMAC- Fe^{3+} by circulating a desorbing agent, a solution of 0.1M EDTA, through the monolith system. There are various known factors that are thought to determine desorption rate of bound Fe^{3+} , such as an extended hydration of metal ions, the polymer microstructure, and the binding

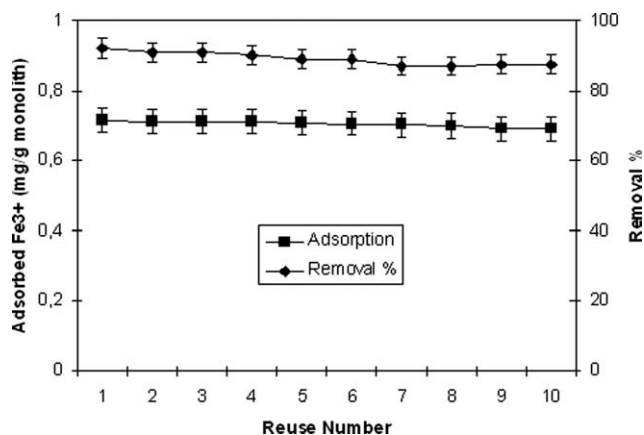


Figure 6 Adsorption–desorption cycle of PHEMAC-Fe³⁺. Experimental conditions are flow rate, 0.5 mL/min; Fe³⁺ ion concentration, 30 mg/L; adsorption buffer, 0.1M acetate buffer; pH, 5.0; desorption agent, 0.1 EDTA; V_{total} , 50 mL; $m_{\text{dry monolith}}$, 0.35 g; T , 20°C.

strength of metal ions. In this study, desorption time was found to be 30 min on the average. Desorption ratios were repeatedly determined to be as high 91% (Figure 6). Eventhough the adsorption–desorption cycles for the PHEMAC-Fe³⁺ column were repeated ten times, the adsorption capacity of the recycled column was maintained at 90% level at the 10th cycle. It is therefore quite likely that the PHEMAC-Fe³⁺ monoliths can be used many times without decreasing their adsorption capacities significantly.

CONCLUSION

Molecularly imprinted polymers (MIPs) are materials that can be readily tailored with selectivity and affinity for guest molecules.^{30–33} Accordingly, MIPs have been utilized in many analytical applications that require molecular recognition, including sensors, adsorbents, immuno-type assays, and chromatographic stationary phases.^{34–37} They possess several advantages over their biological counterparts, including low cost, simple and convenient preparation, storage stability, repeated operations without loss of activity, high mechanical strength, durability to heat and pressure, and applicability in harsh chemical media.^{38–40} Microporous PHEMA films carrying Cibacron blue F3GA, Congo red, and ferritin were prepared by Yavuz et al.⁴¹ for iron ion removal from human plasma. The maximum amounts of Fe(III) removed from human plasma by Cibacron blue F3GA, Congo red, and ferritin attached PHEMA films were 3.80, 4.41, and 8.1 $\mu\text{g}/\text{cm}^2$, respectively. Karabörk et al.⁴² prepared inorgano-organometallic Fe³⁺ ion imprinted polymer nanocomposite traps using methacryloylamidoantipyrine as functional monomer. Their maximum Fe³⁺ binding capacity was 78.5 mg/g and the selectivity of the ad-

sorbent was 5.28, 11.4, 15.8, and 72.6 times higher with respect to Al³⁺, Cu²⁺, Co²⁺, and Zn²⁺ ions, respectively. Chang et al.⁴³ prepared Fe(III)-imprinted amino functionalized silica gel, and their maximum static adsorption capacity for Fe(III) was 25.21 mg/g with a 49.9 times higher selectivity than Cr(III). Aslyüce et al.⁴⁴ used iron imprinted PHEMAC monolithic cryogels to remove Fe(III) ions from human plasma. Their maximum adsorption capacity was 75 $\mu\text{g}/\text{g}$ and the selectivity coefficients of the adsorbent were 12.6 and 2.3 for Cd²⁺ and Ni²⁺, respectively. Yavuz et al.⁴⁵ investigated Fe³⁺ removal performance of Fe³⁺ imprinted poly(HEMA-MAGA) beads and poly(HEMA-MAGA) membranes⁴⁶ from iron overdosed human plasma. Their adsorption capacity was 92.6 $\mu\text{mol}/\text{g}$ for beads and 164.2 $\mu\text{mol}/\text{g}$ for membranes. Karabörk et al.⁴⁷ prepared Fe(III) imprinted poly(MAAP-EGDMA) beads with Fe(III) adsorption capacity of 29.32 mg/g. Thermosensitive polymers were also used for the preparation of iron imprinted adsorbents. Utku et al.⁴⁸ prepared thermosensitive Fe(III) imprinted poly(NIPA-MAC) particles for Fe(III) removal from human plasma. They reached about 40 mg/g Fe(III) adsorption capacity. In this study, Fe³⁺-imprinted PHEMA based monolith containing *N*-methacryloyl-(L)-cysteine methyl ester (MAC) was prepared and was applied for the selective removal of Fe³⁺ ions from aqueous solutions. The specific surface area increased after template removal as a result of formation of cavities. The adsorption difference between the PHEMAC and PHEMAC-Fe³⁺ monoliths is most probably because of geometric shape affinity (or memory) of Fe³⁺ ions toward the cavities in the PHEMAC-Fe³⁺ structure. The Langmuir adsorption model can be applied in this affinity adsorbent system. The relative selectivity coefficient is an indicator to express an adsorption affinity of recognition sites to the imprinted Fe³⁺ ions. A significant increase was observed in the selectivity of PHEMAC-Fe³⁺ monolith when the adsorbent was prepared in the presence of the target ion. Finally, the PHEMAC-Fe³⁺ monolith can be used many times without decreasing their adsorption capacities significantly.

References

1. Wulff, G. *Angew Chem Int Ed Engl* 1995, 34, 1812.
2. Ramstrom, O.; Mosbach, K. *Curr Opin Chem Biol* 1999, 3, 759.
3. Andersson, L. I.; Nicolla, I. A. *J Chromatogr B* 2004, 804, 1.
4. Striegler, S. *J Chromatogr B* 2004, 804, 183.
5. Cui, A.; Singh, A.; Kaplan, D. L. *Biomacromolecules* 2002, 3, 1353.
6. Piletsky, S. A.; Piletskaya, E. V.; Panasyuk, T. L.; El'skaya, A. V.; Levi, R.; Karube, I.; Wulff, G. *Macromolecules* 1998, 31, 2137.
7. Ozcan, A. A.; Say, R.; Denizli, A.; Ersoz, A. *Anal Chem* 2006, 78, 7253.
8. Bereli, N.; Andaç, M.; Baydemir, G.; Say, R.; Galaev, I. Y.; Denizli, A. *J Chromatogr A* 2008, 1190, 18.

9. Ye, L.; Mosbach, K. *J Am Chem Soc* 2001, 123, 2901.
10. Zhang, L.; Cheng, G.; Fu, C. *Funct Polym* 2003, 56, 167.
11. Liu, Y.; Chang, X.; Wang, S.; Guo, Y.; Din, B.; Meng, S. *Anal Chim Acta* 2004, 519, 173.
12. Cormack, P. A. G.; Mosbach, K. *React Funct Polym* 1999, 41, 115.
13. Andac, M.; Ozyapi, E.; Senel, S.; Say, R.; Denizli, A. *Ind Eng Chem Res* 2006, 45, 1780.
14. Say, R.; Ersöz, A.; Denizli, A. *Sep Sci Technol* 2003, 38, 3431.
15. Yoshida, M.; Uezu, K.; Goto, M.; Furusaki, S. *J Appl Polym Sci* 1999, 73, 1223.
16. Biju, V. M.; Gladis, J. M.; Rao, T. P. *Anal Chim Acta* 2003, 478, 43.
17. Rao, T. P.; Daniel, S.; Gladis, J. M. *Trends Anal Chem* 2004, 23, 28.
18. Cao, R.; Gu, Z.; Patterson, G. D.; Armitage, B. A. *J Am Chem Soc* 2004, 126, 726.
19. Ren, Y.; Zhang, M.; Zhao, D. *Desalination* 2008, 228, 135.
20. McCoy, M.; Kalghatgi, K.; Regnier, F. E. *J Chromatogr A* 1996, 743, 221.
21. Altintas, E. B.; Denizli, A. *J Chromatogr B* 2006, 832, 216.
22. Uzun, L.; Say, R.; Denizli, A. *React Funct Polym* 2005, 64, 93.
23. Zou, H.; Huang, X.; Ye, M.; Luo, Q. *J Chromatogr A* 2002, 954, 5.
24. Uzun, L.; Yavuz, H.; Say, R.; Ersöz, A.; Denizli, A. *Ind Eng Chem Res* 2004, 43, 6507.
25. Özkara, S.; Say, R.; Andaç, C.; Denizli, A. *Ind Eng Chem Res* 2008, 47, 7849.
26. Dai, S.; Burleigh, M. C.; Shin, Y.; Morrow, C. C.; Barnes, C. E. *Angew Chem Int Ed Engl* 1999, 38, 1235.
27. Finette, G. M. S.; Qui-Ming, M.; Hearn, M. T. W. *J Chromatogr A* 1997, 763, 71.
28. Oncel, S.; Uzun, L.; Garipcan, B.; Denizli, A. *Ind Eng Chem Res* 2005, 44, 7049.
29. Denizli, A.; Piskin, E. *J Biochem Biophys* 2001, 49, 391.
30. Say, R.; Birlik, E.; Ersöz, A.; Yilmaz, F.; Gedikbey, T.; Denizli, A. *Anal Chim Acta* 2003, 480, 251.
31. Biju, V. M.; Gladis, J. M.; Rao, T. P. *Anal Chim Acta* 2003, 478, 43.
32. Ersöz, A.; Denizli, A.; Özcan, A.; Say, R. R. *Biosens Bioelectron* 2005, 20, 2197.
33. Andaç, M.; Say, R.; Denizli, A. *J Chromatogr B* 2004, 811, 119.
34. Lavignac, N.; Allender, C. J.; Brain, K. R. *Anal Chim Acta* 2004, 510, 139.
35. Haginaka, J. *Bioseparation* 2002, 10, 337.
36. Uzun, L.; Say, R.; Unal, S.; Denizli, A. *J Chromatogr B* 2009, 877, 181.
37. Uzun, L.; Say, R.; Unal, S.; Denizli, A. *Biosens Bioelectron* 2009, 24, 2878.
38. Demirçelik, A. H.; Andaç, M.; Andaç, C. A.; Say, R.; Denizli, A. *J Biomater Sci Polym Ed* 2009, 20, 1235.
39. Andaç, M.; Mirel, S.; Say, R.; Şenel, S.; Ersöz, A.; Denizli, A. *Int J Biol Macromol* 2007, 40, 159.
40. Vlatakis, G.; Andersson, L. I.; Müller, R.; Mosbach, K. *Nature* 1993, 361, 645.
41. Yavuz, H.; Arica, Y.; Denizli, A. *J Appl Polym Sci*, 2001, 82, 186.
42. Karabörk, M.; Ersöz, A.; Denizli, A.; Say, R. *Ind Eng Chem Res* 2008, 47, 2258.
43. Chang, X.; Jiang, N.; Zheng, H.; He, Q.; Hu, Z.; Zhai, Y.; Cui, Y. *Talanta*, 2007, 71, 38.
44. Asliyüce, S.; Bereli, N.; Uzun, L.; Onur, M. A.; Say, R.; Denizli, A. *Purif Technol* 2010, 73, 243.
45. Yavuz, H.; Say, R.; Denizli, A. *Mater Sci Eng C* 2005, 25, 521.
46. Yavuz, H.; Andaç, M.; Uzun, L.; Say, R.; Denizli, A. *Int J Artif Org* 2006, 29, 900.
47. Karabörk, M.; Ersöz, A.; Ersöz, E.; Say, R. *Hacettepe J Biol Chem* 1997, 35, 135.
48. Utku, S.; Yilmaz, E.; Türkmen, D.; Uzun, L.; Garipcan, B.; Say, R.; Denizli, A. *Hacettepe J Biol Chem* 2008, 36, 291.